Dynamics of persistent collision complexes in molecular beam reactive scattering

Roger Grice[a]

[a] Chemistry Department, University of Manchester, Manchester, England

PLEASE SCROLL DOWN FOR ARTICLE

Dynamics of persistent collision complexes in molecular beam reactive scattering

by ROGER GRICE

Chemistry Department, University of Manchester,
Manchester M13 9PL, England

New microcanonical theories for the angular distributions of reactive scattering arising from long-lived collision complexes and their application to a wide range of transition state geometries are reviewed. Transition states formed at the top of centrifugal barriers on potential energy surfaces without a potential energy barrier are well described by symmetric top transition states, provided that the loosening of bending mode vibrations into product rotation is included. A phase space description appropriate for collisions at small impact parameters can be incorporated into a consistent mathematical description. Tight transition states formed at the top of a potential energy barrier and involving H atom displacement are described by an asymmetrical top transition state theory which includes all the symmetric top configurations as limiting cases. However the effects of transition state flexibility rapidly obscure the observable consequences of preferred geometry for directions of dissociation away from the principal axes. These theories are used to explore the effects of structural isomerism of collision complexes in studies of a wide range of F and O atom abstraction and displacement reactions, where the structure and interconversion of highly vibrationally excited complexes is related to the nature of the chemical bonding involved.

1. Introduction

Molecular beam studies of chemical reaction dynamics have assembled a large body of experimental results, but the understanding which has been gained from these data rests primarily upon a limited range of dynamical models [1]. These allow the observed scattering to be related to the underlying structure of the reaction potential energy surface but have been largely qualitative in their application. Long-lived complexes were first identified in the exchange reactions of alkali atoms and alkali halide molecules by Miller, Safron and Herschbach [2] and the observed reactive scattering was interpreted using the Halpern–Strutinski model [3] for nuclear fission. This provides an appropriate mathematical form for the description of angular distributions of reactive scattering arising from long-lived collision complexes located in a well on the reaction potential energy surface as illustrated in figure 1, where energy is randomized over internal degrees of freedom of the complex and of the transition state for its dissociation to form reaction products. However, the Halpern–Strutinski model erroneously assumes a canonical statistical distribution over the internal degrees of freedom of the transition state which postulates the existence of a heat bath and cannot be appropriate under the isolated collision conditions of a molecular beam scattering experiment. For this reason the parameters associated with the use of the Halpern–Strutinski model are phenomenological in character and are not specifically related to the structure and energetics of the transition state. This review will describe new microcanonical theories of scattering from persistent collision complexes which now allow the observed
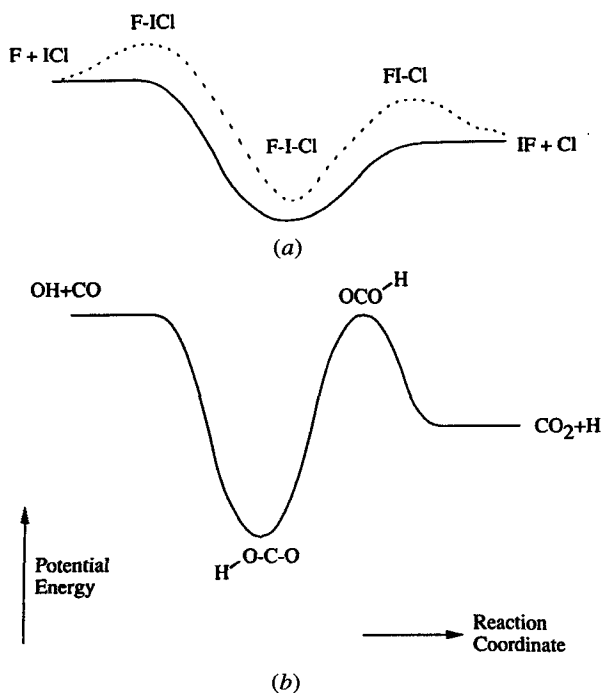
Figure 1. Potential energy profiles for (*a*) the F + ICl reaction showing a minimum without a potential energy barrier (*b*) the OH + CO reaction with both a minimum and a potential energy barrier to dissociation. Solid curve for collisions at small impact parameters with low initial orbital angular momentum $L \sim 0$; broken curve for collisions at large impact parameters with high initial orbital angular momentum $L \sim 100-200\,\hbar$.

scattering to be related to the geometry and energetics of the product transition state explicitly.

2. Microcanonical theory for symmetric top transition states

The microcanonical theory assumes a uniform statistical distribution over all accessible internal quantum states of the collision complex and all transition states which lead to dissociation to reaction products or back to reactants, subject to conservation of the total energy and angular momentum of the collision. If the life-time of the collision complex is long compared with its rotational period, the spatial distribution of the principal axis of a symmetric top transition state for dissociation of the complex may be characterized by the cosine of the helicity angle α lying between the principal axis and the total angular momentum. For a given value of $\cos\alpha$, the directions of the symmetric top axis are uniformly distributed on a cone about the total angular momentum. The total angular momentum may be equated with the initial orbital angular momentum L, which lies perpendicular to the initial relative velocity v, in the common case that L is very much greater than the rotational angular momentum J of the reactant molecule as shown in figure 2. The microcanonical distribution for the square of the cosine of the helicity angle α is then given according to Jarvis and Grice [4] by

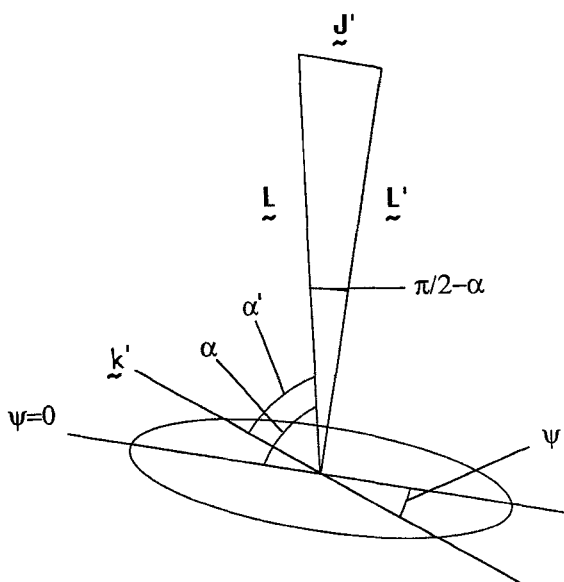$$P(\cos^2\alpha) \propto (1 - a^2\cos^2\alpha)^{s-1}, \tag{1}$$

Figure 2. Symmetry axis of a symmetric top transition state at angle $\psi = 0$ and final relative velocity v' at angle ψ with respect to the total angular momentum represented by the initial orbital angular momentum L and the angular momentum components L' perpendicular to and J' parallel to the top axis. The helicity angle between the total angular momentum and the top axis is denoted by α and the helicity angle for the final relative velocity by α'.

for $\cos^2 \alpha \leqslant 1/a^2$ and zero otherwise, where

$$a^2 = (\mu/\mu')[(I_2^+/I_1^+) - 1]/[1 - (\mu/\mu') + \Delta D_0/E], \qquad (2)$$

and s denotes the number of internal degrees of freedom of the transition state; μ, μ' the initial and final reduced masses; I_1^+, I_2^+ the moments of inertia parallel and perpendicular to the top axis; E the initial translational energy and ΔD_0 the reaction exoergicity. Initially the direction of dissociation of the transition state will lie along the top axis denoted by $\psi = 0$ in figure 2 but the decline in bonding forces as the transition state dissociates will allow the final relative velocity v' to move away from this direction. If it is assumed that the direction of v' becomes uniformly distributed over the angle ψ lying in the plane perpendicular to the component of angular momentum L', in figure 2, the distribution of the cosine of the helicity angle α' lying between the final relative velocity v' and the total angular momentum becomes

$$P(\cos \alpha') \propto (1 - a^2 \cos^2 \alpha')^{s - 1/2}, \qquad (3)$$

for $\cos^2 \alpha' \leqslant 1/a^2$ and zero otherwise. The product angular distribution is then given by the integral

$$I(\theta) = \frac{2}{\pi} \int_0^{\min} \frac{(1 - a^2 \cos^2 \alpha')^{s - 1/2}}{(\sin^2 \theta - \cos^2 \alpha')^{1/2}} \, \mathrm{d} \cos \alpha', \qquad (4)$$

where θ denotes the scattering angle and $\min = 1/a$ or $\sin \theta$ whichever is the less. Analytical expressions for the integral of equation (4) have been given up to $s = 15/2$ [4–6]. This microcanonical formulation describes the large impact parameter limit of the reactive scattering with the transition state being located at the top of the centrifugal

barrier in the exit valley of the reaction potential energy surface as shown in figure 1. In the case of a prolate top transition state, this yields an angular distribution peaking in the forward and backward directions and with the initial orbital angular momentum being disposed mainly into product orbital angular momentum $L \sim L'$. However, in the small impact parameter limit, the distribution of the angle $\pi/2 - \alpha$ lying between L and L' can be calculated from phase space theory [7, 8]. If the calculated distribution of $\cos(\pi/2 - \alpha)$ is fitted by polynomial least squares to a three term expansion [9]

$$P(\sin\alpha) = c_0 + c_2 \sin^2\alpha + c_4 \sin^4\alpha, \tag{5}$$

then this may be transformed to the distribution

$$P(\cos\alpha') = c_0 + \tfrac{1}{2}c_2 \sin^2\alpha' + \tfrac{3}{8}c_4 \sin^4\alpha', \tag{6}$$

where the second and third terms correspond to equation (3) with $a^2 = 1$ and $s = 3/2$, $5/2$. Consequently the individual terms for the angular distribution are also given by the analytical expressions derived from equation (4) in the limit $a^2 = 1$. The extended microcanonical theory [9] uses two phase space terms and one microcanonical term to give a three-term expansion which matches the two forms at the impact parameter corresponding to $a^2 = 1$. The extended microcanonical theory has been tested over a wide range of fluorine atom reactions in which iodine atom abstraction occurs via a persistent collision complex

$$F + IR \rightarrow F\text{–}I\text{–}R \rightarrow IF + R, \tag{7}$$

where the moment of inertia ratio and energetics of the product transition state can be varied systematically by altering the identity of the hydrocarbon radical R and the initial translational energy E. High-resolution differential reaction cross-sections have been measured which are consistent with the predictions of the microcanonical theory. The iodomethane reaction $R = CH_3$ requires [10] only the single microcanonical term alone with the parameter a^2 averaged over impact parameter, to describe the sharp forward and backward peaking which results from reaction over a high centrifugal barrier

$$a^2 = [(I_2^+/I_1^+) - 1]/\{[(1 + \Delta D_0/E)\mu' L_m^2/\mu L^2] - 1\}. \tag{8}$$

The t-butyliodide reaction $R = C(CH_3)_3$ with a greatly decreased moment of inertia ratio [6] gives lower values of the parameter a^2 and all three terms of the extended microcanonical expansion make significant contributions to the mildly forward and backward peaked angular distribution. The reactions with $R = C_2H_5$, C_3H_7, $CH(CH_3)_2$ provide intermediate cases [5] with the angular distribution for $F + C_2H_5I$ being shown in figure 3.

In all of these cases the $L \gg J$ limit is well fulfilled, however, in the iodobenzene reaction $R = C_6H_5$ the heavy reactant molecule [11] carries a significant though still minor component of the total angular momentum $J_{mp}/L_m \sim 0.1$. In this case the final integral of equation (4) is replaced by

$$I(\theta) = \frac{1}{\pi} \int_{min}^{max} \frac{P(\cos\alpha')\,d\cos\alpha'}{(\sin^2\theta - \cos^2\gamma + 2\cos\gamma\cos\theta\cos\alpha' - \cos^2\alpha')^{1/2}}, \tag{9}$$

where $min/max = \cos(\theta \pm \gamma)$ and $\cos\gamma = J_{mp}/L_m$ with $J_{mp} \ll L_m$. For $F + C_6H_5I$, the three-term expansion of equation (6) gives a good polynomial least squares fit to the phase space $P(\sin\alpha)$ distribution and the inclusion of the reactant angular
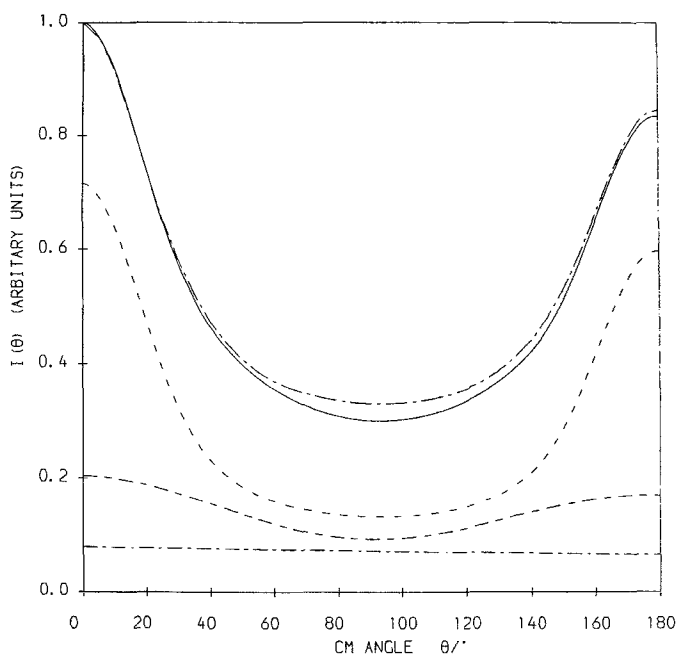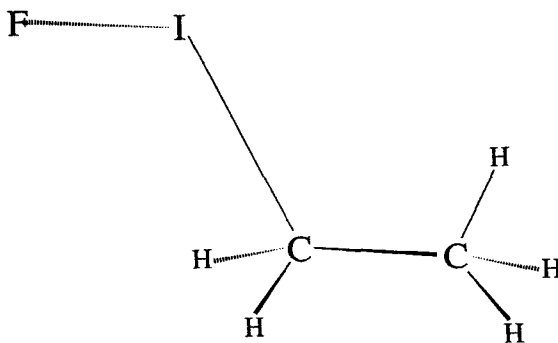
Figure 3. (*a*) Angular distribution for F + C_2H_5I at initial translational energy $E = 38 \, kJ \, mol^{-1}$ calculated from the extended microcanonical model (solid curve) compared with the experimental distribution (broken curve). The components of the three-term expansion are shown separately by broken curves, with the microcanonical component being the most sharply peaked. (*b*) Product transition state in the limiting *trans* configuration for F + C_2H_5I with free rotation about the extended I–F bond.

momentum has only a very modest effect on the broad angular distribution predicted in agreement with the experimental angular distribution.

In all of these reactions, the product translational energy distribution is much less sensitive to the structure of the product transition state and can be calculated adequately using phase space theory. For reactions with sharply forward and backward peaked angular distributions, the product translational energy distribution for sideways scattering represents an average over the full range of impact parameters, while the

forward and backward scattering is representative only of the largest impact parameters [12]. Indeed the reaction

$$F + ICl \rightarrow FICl \rightarrow IF + Cl \tag{10}$$

changes [13] from a purely microcanonical description at high initial translational energy $E \sim 34\,kJ\,mol^{-1}$ to a purely phase space description at lower initial translational energy $E \sim 12\,kJ\,mol^{-1}$.

3. Microcanonical theory for asymmetric top transition states

The transition states described in the preceding section are located at the top of a centrifugal barrier in the exit valley of the potential energy surface and as the initial orbital angular momentum decreases the transition state moves out to the asymptotic reaction products. However when a long-lived collision complex dissociates via a transition state located at the top of a potential energy barrier on the potential energy surface, the geometrical constraints become much tighter and when dissociation involves the displacement of a light hydrogen atom the geometry of the transition state is reflected in the angular distribution of reactive scattering. The precessional motion of the collision complex and hence the resulting distribution of asymmetric top transition states generates a distribution of the cosine of the helicity angle for dissociation along each of the three principal axes [14] which can be expressed as an integral

$$P(\cos \alpha') = \int_{-1}^{1} [(p - qx)^{s-1}/\pi(1 - x^2)^{1/2}]\,dx, \tag{11}$$

depending on two parameters p and q, which for the c-axis are

$$p = 1 - \left[\frac{L^2}{4} \left(\frac{1}{I_a} + \frac{1}{I_b} - \frac{2}{I_c} \right) \frac{\sin^2 \alpha'}{(E_{tot} - L^2/2I_c)} \right], \tag{12a}$$
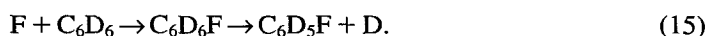
$$q = \frac{L^2}{4} \left(\frac{1}{I_a} - \frac{1}{I_b} \right) \frac{\sin^2 \alpha'}{(E_{tot} - L^2/2I_c)}. \tag{12b}$$

Analytical expressions for $P(\cos \alpha')$ have been given for $s \leqslant 18$ [14, 15]. The resulting integrals for the product angular distribution

$$I(\theta) = \frac{2}{\pi} \int_{0}^{\sin \theta} \frac{P(\cos \alpha')\,d\cos \alpha'}{(\sin^2 \theta - \cos^2 \alpha')^{1/2}} \tag{13}$$

are not readily integrated analytically, but can be evaluated numerically. The resulting angular distributions show that dissociation along the a principal axis of least moment of inertia I_a always yields scattering peaked in the forward and backward directions, while dissociation along the c principal axis of greatest moment of inertia I_c always yields scattering peaked in sideways direction. Dissociation along the b principal axis of intermediate moment of inertia I_b yields forward and backward scattering in the oblate top limit [16] and sideways scattering in the prolate top limit [17].

Sideways peaked angular distributions are observed for the H and D atom displacement reactions of F atoms with C_2H_4 and C_6D_6 molecules [18–22]

$$F + C_2H_4 \rightarrow CH_2-CH_2F \rightarrow C_2H_3F + H, \tag{14}$$

$$F + C_6D_6 \rightarrow C_6D_6F \rightarrow C_6D_5F + D. \tag{15}$$

Ab initio calculations [23] for the dissociation of the fluoroethyl radical in equation (14)

show the H atom departing parallel to the *c* axis of the transition state as shown in figure 4. Calculations with this asymmetric top transition state yield [14] a sideways peaked angular distribution in good agreement with the experimental angular distribution in figure 4. Indeed this is also the case for the $F + C_6D_6$ angular distribution when an analogous transition state configuration is again employed. While it might be expected that H atom displacement in a direction lying between the principal axes of an asymmetric top transition state might give rise to intermediate conical scattering, model calculations [24] on the dissociation of the HOCO collision complex in the reaction

$$OH + CO \rightarrow HOCO \rightarrow CO_2 + H \qquad (16)$$
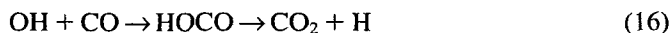
indicate that this is unlikely to be observed in practice. The transition state geometry shown in figure 5 has the direction of H atom displacement lying between the *a* and *b*-axes, but the range of transition state bending angles about the preferred value $\beta = 45°$ generated by bending mode excitation and by the recoil of the departing H atom against the product CO_2 molecule yields a mildly forward and backward peaked angular distribution in accord with the experimental angular distribution [25] even in this exceptionally favourable case of an asymmetrical top which approaches the linear rotator limit.

4. Life-time of collision complexes and dependence on initial transitional energy

The life-time distribution of the BrII collision complex in the exchange reaction

$$Br + I_2 \rightarrow BrII \rightarrow IBr + I \qquad (17)$$

has been measured directly by femtosecond laser spectroscopy [26] and follows the exponential decay law expected for unimolecular decomposition. Employment of this distribution law in the osculating complex model [27] allows the decay life-time τ of the collision complex to be determined relative to the rotational period τ_r of complexes formed in large impact parameter collisions from the relative magnitude of the forward and backward scattering

$$I(0°)/I(180°) = \exp(\tau_r/2\tau). \qquad (18)$$

The ratios of the life-times of the FI*R* collision complexes in equation 7 to their rotational periods have been estimated [28] by the Rice–Ramsperger–Kassel–Marcus (RRKM) formula [29, 30]

$$\frac{\tau}{\tau_r} \approx \frac{L_m}{2\pi I_2^* \bar{v}} \left(\frac{E + \Delta D_0 + E_0 - I_2^+ E_{pk}'/I_2^*}{E + \Delta D_0 - E_{pk}'} \right)^{s-1}, \qquad (19)$$

where I_2^* denotes the larger moment of inertia of the FI*R* complex and E_{pk}' the peak product translational energy. The bond dissociation energies E_0 of the FI*R* complexes with respect to reaction products were determined by measuring the translational energy threshold for the endoergic reactions

$$F_2 + I R \rightarrow FI R + F. \qquad (20)$$

The life-time ratios calculated from equation (19) give good agreement with the ratios estimated from the experimental angular distributions of reactive scattering using equation (18), when the effective number of internal degrees of freedom estimated from the microcanonical theory for the IF product angular distribution are again employed. In each case the effective number of degrees of freedom corresponds to counting only the low-frequency modes which are classically excited in the FI–*R* product transition state. As the life-time of the FI*R* collision complex in the allyl iodide reaction $R = C_3H_5$

R. Grice
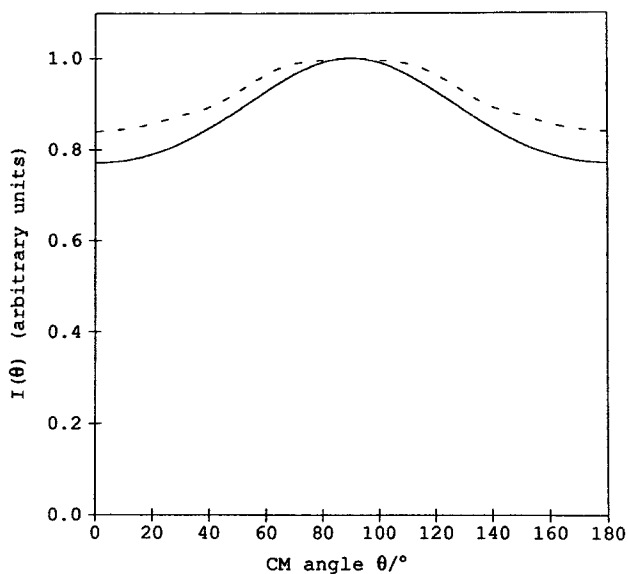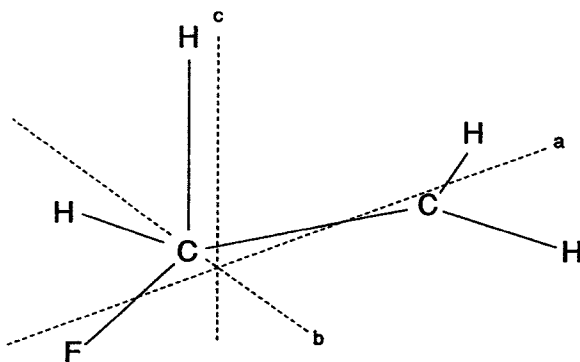
Figure 4. (a) Angular distribution for $F + C_2H_4$ at initial translational energy $E = 51 \, kJ \, mol^{-1}$ calculated from the asymmetric top model (solid curve) compared with the experimental distribution (broken curve). (b) Product transition state for $F + C_2H_4$ with H atom displacement parallel to the c principal axis.
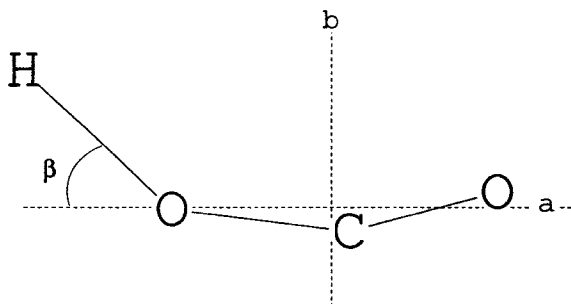
Figure 5. Product transition state for the OH + CO reaction with H atom displacement at a preferred bending angle $\beta = 45°$ lying between the a and b principal axes.

$^3A''$ pathway

Br Br ⟹ OBr↔Br ⟹ BrO + Br

O

intersystem
crossing ⟱

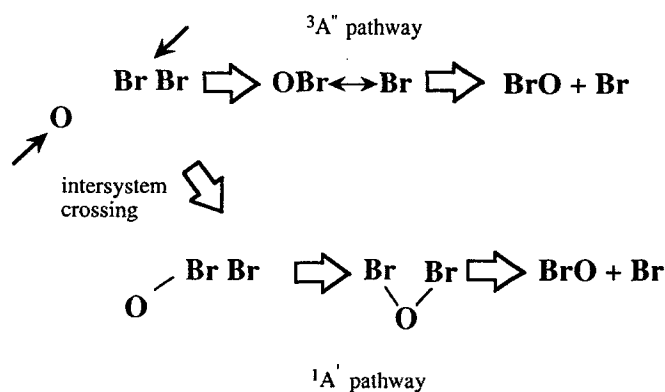Br Br ⟹ Br Br ⟹ BrO + Br
O   O

$^1A'$ pathway

Figure 6. Reactant transition state for $O(^3P) + Br_2$ leading to direct dissociation on the $^3A''$ potential energy surface or intersystem crossing to the $^1A'$ surface followed by dissociation via a bent BrOBr complex.

becomes less than the rotational period [31], energy is no longer randomized over the internal modes of the FIR complex. Nonetheless the overall distribution of internal energy which determines the product angular and translational energy distributions, is compatible with microcanonical theory for a lower number of active degrees of freedom.

However this tendency toward increasing forward scattering with increasing initial translational energy is not uniformly observed in the reactions of $O(^3P)$ atoms with halogen and alkyl iodide molecules. In the case of the reactions [32,33]

$$O(^3P) + Br_2 \rightarrow BrO + Br, \tag{21}$$

and [34]

$$O(^3P) + IR \rightarrow IO + R, \tag{22}$$

the scattering increases in the backward hemisphere with increasing initial translational energy. This reflects the role of two potential energy surfaces as shown for $O + Br_2$ in figure 6, with motion over the triplet $^3A''$ surface giving rise to scattering in the backward hemisphere while motion on the underlying singlet $^1A'$ surface gives long-lived collision dynamics. Intersystem crossing from the triplet to the singlet potential energy surface is induced by spin–orbit interaction at the seam of intersection in the OBrBr configuration in the entrance valley. Analysis of the conical scattering observed at high initial translational energy for $O + Br_2$ using the direct interaction with product repulsion (DIPR) model [35,36] indicates a bent OBrBr geometry with interbond angle $\beta \sim 130°$ for the transition state on the $^3A''$ potential energy surface. Intersystem crossing to the $^1A'$ surface occurs in this configuration with a dative covalent bond $O \leftarrow Br–Br$ giving some stability but with the more stable bent Br–O–Br configuration with a divalent O atom giving rise to long-lived complex dynamics. In the case of the $O + IR$ reactions [34] similar considerations apply but it appears that the dative covalency $O \leftarrow I–R$ is sufficiently stable to give rise to long-lived complex dynamics on the singlet surface. Indeed evidence has recently been obtained [37] for the subsidiary stability of the OBrH configuration of the HOBr collision complex in the reaction

$$O(^1D) + HBr \rightarrow BrO + H, \tag{23}$$

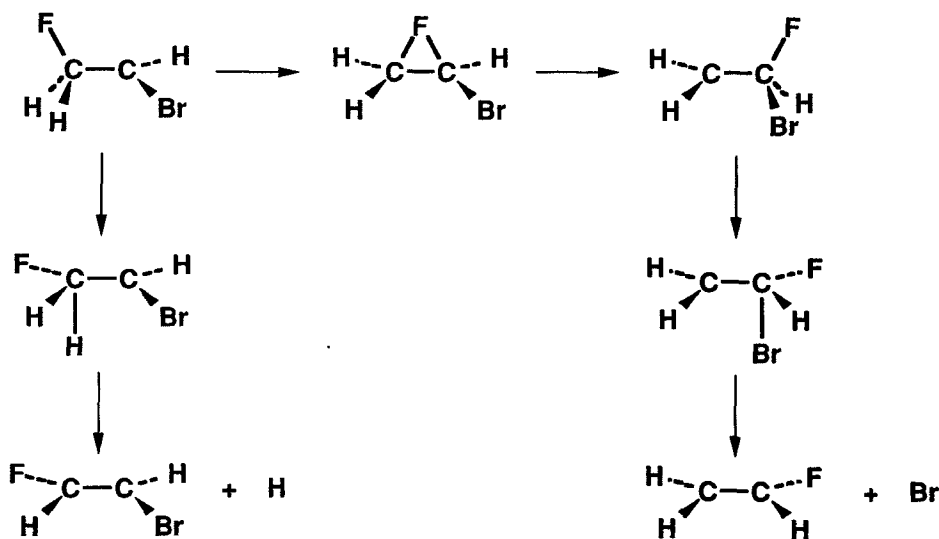which takes place on the singlet potential energy surface [38].

Figure 7. Isomers of the fluorobromoethyl radical intermediate and transition states for H, Br atom displacement and F atom migration involved in the F + C_2H_3Br reaction. Reprinted from [15] by permission of the American Chemical Society.

The structural isomerism of long-lived collision complexes has been investigated explicitly in the reactions of F atoms with vinyl, allyl and aryl halide molecules. Addition of the F atom to the C=C double bond of vinyl bromide gives rise to both H atom and Br atom displacement [15]

$$F + C_2H_3Br \rightarrow CHFCHBr + H$$
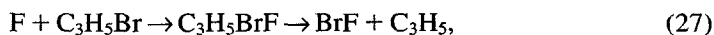$$\rightarrow C_2H_3F + Br, \tag{24}$$
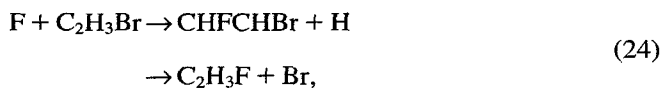
depending on the isomer of the fluorobromoethyl radical which is formed as the collision intermediate. However the H atom displacement which follows addition to the CH_2 group is also in competition with F atom migration to the CHBr group followed by Br atom displacement as shown in figure 7. Similarly the F atom addition to the benzene ring of C_6H_5I yields both H atom and I atom displacement.

$$F + C_6H_5I \rightarrow C_6H_4FI + H$$
$$\rightarrow C_6H_5F + I. \tag{25}$$

However F atom addition to the C=C double bond of allyl bromide or iodide molecules gives rise only to halogen atom displacement and it is suggested that isomeric allyl fluoride and fluorocyclopropane product molecules are both formed [39, 40]

$$F + C_3H_5X \rightarrow C_3H_5F + X$$
$$\rightarrow cyclo\, C_3H_5F + X. \tag{26}$$
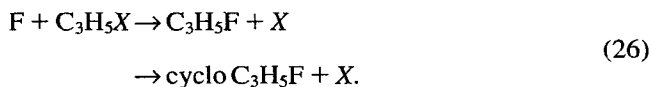
Remarkably the halogen atom abstraction pathways are also observed in the reactions of F atoms with allyl bromide and iodobenzene molecules [11]

$$F + C_3H_5Br \rightarrow C_3H_5BrF \rightarrow BrF + C_3H_5, \tag{27}$$

$$F + C_6H_5I \rightarrow C_6H_5IF \rightarrow IF + C_6H_5. \tag{28}$$

In both cases the halogen atom abstraction pathways of equations (27, 28) are much less exoergic than the corresponding displacement pathways of equations (25, 26) and the intermediate collision complexes have very long life-times. Clearly a potential energy barrier must impede the F atom bonded to the halogen atom from migrating to the $C=C$ double bond of the C_3H_5 group or the π system of the C_6H_5 group in each case. Evidently charge transfer interaction [41] of the form RX^+F^- inhibits the migration of the F atom to alternative electrophilic centres.

5. Conclusions and future prospects

The molecular beam reactive scattering measurements outlined above, show the way in which the chemical bonding theory of organic and inorganic molecules applies to the structure of the intermediate complexes and transition states on the reaction potential energy surfaces. The dynamical models described allow a systematic identification of these features of the potential energy surface and provide a dynamical average structure for the transition states in the absence of individual quantum state resolution. Quantum dynamical calculations [42] have been used to assign vibrational quantum numbers to the quasi-bound resonance states for the HOCO complex of equation (16). Currently these calculations are of reduced dimensionality so that the angular distribution of reactive scattering is not predicted correctly [24, 25, 43]. Even so, the preferred decay pathway of each resonance is found to depend upon its quantum numbers and hence on the location of the wavefunction on the potential energy surface. This illustrates the way in which statistical behaviour arises [44–46] from the energy overlap of quasi-bound resonances. Clearly the phenomenon of persistent collision complexes continues to stimulate that interaction of theory and experiment which is such a rich feature of the field of chemical reaction dynamics.

Acknowledgments

References

[1] LEVINE, R. D., and BERNSTEIN, R. B., 1987, *Molecular Reaction Dynamics and Chemical Reactivity* (Oxford University Press).
[2] MILLER, W. B., SAFRON, S. A., and HERSCHBACH, D. R., 1967, *Discuss. Faraday Soc.*, **44**, 108.
[3] HALPERN, I., and STRUTINSKI, V. M., 1958, *Proceeding Second International Conference on Peaceful Uses of Atomic Energy* (Geneva) (New York: United Nations), p. 408.
[4] JARVIS, R. D., and GRICE, R., 1988, *Molec. Phys.*, **65**, 1205.
[5] HARKIN, J. J., JARVIS, R. D., SMITH, D. J., and GRICE, R., 1990, *Molec. Phys.*, **71**, 323.
[6] HARKIN, J. J., SMITH, D. J., and GRICE, R., 1991, *Molec. Phys.*, **72**, 95.
[7] PECHUKAS, P., LIGHT, J. C., and RANKIN, C., 1966, *J. chem. Phys.*, **44**, 794.
[8] LIN, J., and LIGHT, J. C., 1966, *J. chem. Phys.*, **59**, 2545.
[9] JARVIS, R. D., HARKIN, J. J., SMITH, D. J., and GRICE, R., 1990, *Chem. Phys. Lett.*, **167**, 190.
[10] JARVIS, R, D., FIRTH, N. C., SMITH, D. J., and GRICE, R., 1990, *J. chem. Soc. Faraday Trans.*, **86**, 2059.
[11] WANG, J. J., ZHU, Z. Z., SMITH, D. J., and GRICE, R., 1994, *J. phys. Chem.*, **98**, 10787.
[12] STEELE, T. A., BRADSHAW, N., and GRICE, R., 1985, *Molec. Phys.*, **56**, 1117.
[13] JARVIS, R. D., WHITE, R. W. P., ZHU, Z. Z., SMITH, D. J., and GRICE, R., 1992, *Molec. Phys.*, **75**, 587.
[14] SMITH, D. J., and GRICE, R., 1991, *Molec. Phys.*, **73**, 1371.

[15] ZHU, Z. Z., SMITH, D, J., and GRICE, R., 1994, *J. phys. Chem.*, **98**, 4003.
[16] JARVIS, R. D., and GRICE, R., 1989, *Molec. Phys.*, **66**, 675.
[17] JARVIS, R. D., LAMING, G. J., and GRICE, R., 1990, *Molec. Phys.*, **70**, 667.
[18] PARSON, J. M., SHOBATAKE, K., LEE, Y. T., and RICE, S. A., 1973, *Faraday Discuss. Chem. Soc.*, **55**, 344.
[19] PARSON, J. M., and LEE, Y. T., 1972, *J. chem. Phys.*, **56**, 4658.
[20] FARRAR, J. M., and LEE, Y. T., 1976, *J. chem. Phys.*, **65**, 1414.
[21] ROBINSON, G. N., CONTINETTI, R. E., and LEE, Y. T., 1990, *J. chem. Phys.*, **92**, 275.
[22] SHOBATAKE, K., PARSON, J. M., LEE, Y. T., and RICE, S. A., 1973, *J. chem. Phys.*, **59**, 1427.
[23] SCHLEGEL, H. B., 1982, *J. phys. Chem.*, **86**, 4878.
[24] GRICE, R., and SMITH, D. J., 1993, *Molec. Phys.*, **80**, 1533.
[25] ALAGIA, M., BALUCANI, N., CASAVECCHIA, P., STRANGES, D., and VOLPI, G. G., 1993, *J. chem. Phys.*, **98**, 8341.
[26] SIMS, I. R., GRUEBELE, M., POTTER, E. D., and ZEWAIL, A. H., 1992, *J. chem. Phys.*, **97**, 4127.
[27] FISK, G. A., McDONALD, J. D., and HERSCHBACH, D. R., 1967. *Discuss. Faraday Soc.*, **44**, 228.
[28] WHITE, R. W. P., SMITH, D. J., and GRICE, R., 1993, *J. phys. Chem.*, **97**, 2123.
[29] MARCUS, R. A., 1952, *J. chem. Phys.*, **20**, 359.
[30] MARCUS, R. A., 1965, *J. chem. Phys.*, **43**, 2658.
[31] HARKIN, J. J., SMITH, D. J., and GRICE, R., 1991, *Molec. Phys.*, **72**, 763.
[32] FIRTH, N. C., KEANE, N. W., SMITH, D. J., and GRICE, R., 1988, *Laser Chem.*, **9**, 265.
[33] ROCHFORD, J. J., POWELL, L. J., and GRICE, R., 1995, *J. phys. Chem.* (in the press).
[34] WHITE, R. W. P., SMITH, D, J., and GRICE, R., 1992, *Chem. Phys. Lett.*, **193**, 269.
[35] KUNTZ, P. J., MOK, M. H., and POLANYI, J. C., 1969, *J. chem. Phys.*, **50**, 4623.
[36] LOESCH, H. J., and MÖLLER, J., 1992, *J. chem. Phys.*, **97**, 9016.
[37] BALUCANI, N., BENEVENTI, L., CASAVECCHIA, P., and VOLPI, G. G., 1994, *Can. J. Chem.*, **135**, 888.
[38] BRUNA, P. J., HIRSCH, G., PEYERIMHOFF, S. D., and BUENKER, R. J., 1979, *Can. J. Chem.*, **57**, 1839.
[39] ZHU, Z. Z., SMITH, D. J., and GRICE, R., 1994, *J. phys. Chem.*, **98**, 4008.
[40] ZHU, Z. Z., SMITH, D. J., and GRICE, R., 1994, *Int. J. Mass Spectrom. Ion Proc.*, **135**, 55.
[41] LOEWENSTEIN, L. M., and ANDERSON, J. G., 1987, *J. phys. Chem.*, **91**, 2993.
[42] HERNANDEZ, M. I., and CLARY, D. C., 1994, *J. chem. Phys.*, **101**, 2779.
[43] CLARY, D. C., and SCHATZ, G. C., 1993, *J. chem. Phys.*, **99**, 4578.
[44] SOMEDA, K., NAKAMURA, H., and MIES, F. H., 1994, *Chem. Phys.*, **187**, 195.
[45] SCHERER, N. F., SIPES, C., BERNSTEIN, R. B., and ZEWAIL, A. H., 1990, *J. chem. Phys.*, **92**, 5239.
[46] IONOV, S. I., BRUCKER, G. A., JACQUES, C., VALACHOVIC, L., and WITTIG, C., 1993, *J. chem. Phys.*, **99**, 6553.